

Evolution of solar-type stellar wind

Takeru K. Suzuki^{1,*}

Department of Physics, Nagoya University, Furo-cho, Chikusa, Nagoya, Aichi, 606-8602, Japan

Received XXXX, accepted XXXX

Published online XXXX

Key words Magnetohydrodynamics (MHD), solar wind, stars: chromospheres, stars: winds, waves, turbulence.

By extending our self-consistent MHD simulations for the solar wind, we study the evolution of stellar winds of solar-type stars from early main sequence stage to red giant phase. Young solar-type stars are active and the mass loss rates are larger by up to ~ 100 times than that of the present-day sun. We investigate how the stellar wind is affected when the magnetic field strength and fluctuation amplitude at the photosphere increase. While the mass loss rate sensitively depends on the input energy from the surface because of the global instability related to the reflection and nonlinear dissipation of Alfvénwaves, it saturates at ~ 100 times because most of the energy is used up for the radiative losses rather than the kinetic energy of the wind. After the end of the main sequence phase when the stellar radius expands by ~ 10 times, the steady hot corona with temperature 10^6 K, suddenly disappears. Chromospheric materials, with hot bubbles embedded owing to thermal instability, directly stream out; the red giant wind is not a steady stream but structured outflow.

Copyright line will be provided by the publisher

1 Introduction

The origin of the energy which drives the solar wind is believed to be in the surface convection zone. Turbulent motion associated with the convection excites various modes of waves that propagate upwardly. Magnetic field lines, which are also a consequence of dynamo processes in the surface convective motion (e.g. Yoshimura 1975; Parker 1993), play as a guide for the upgoing waves. Among various types of waves, the Alfvénwave is the most reliable candidate which transfers the energy from the surface convection to the upper region where the solar wind is accelerated because it can travel a longer distance due to the incompressible nature (e.g. Alazraki & Couturier 1971; Belcher 1971; Hollweg 1973).

Alfvénwaves have been extensively studied in the context of driving the solar wind. The dissipation of Alfvén waves is a key to understand the acceleration of the solar wind because it controls the energy and momentum transfer from the waves to the gas. Various types of dissipation mechanisms have been investigated such as ion-cyclotron resonance (e.g. Axford & McKenzie 1992; Kohl et al. 1998), turbulent cascade (e.g. Matthaeus et al. 1996; Verdini & Velli 2007), and the nonlinear mode conversion to compressive modes (e.g. Kudoh & Shibata 1999) by using steady-state models (e.g. Cranmer & van Ballegoijen 2007) or dynamical simulations (e.g. Suzuki & Inutsuka 2005).

Among others, we have carried out magnetohydrodynamical (MHD) simulations covering from the photosphere to the sufficiently outer region where the solar wind is already accelerated (Suzuki & Inutsuka 2005, 2006; Matsumoto & Suzuki 2012). One of the greatest advantage of our dynamical simulations is that the inner boundary is not an ad

hoc ‘coronal base’ or ‘upper chromosphere’ but the photosphere where there are much observational information¹ (e.g. Fujimura & Tsuneta 2009; Matsumoto & Kitai 2010). Therefore, mass loss rate can be directly determined as an output of the surface properties.

This type of wind is not unique to the solar wind. Main sequence stars with mass comparable to or less than the solar mass possess surface convection zones, and the stellar winds emanating from these stars by similar mechanism (e.g. Cranmer & Saar 2011). Observations of astrospheres of low-mass to intermediate-mass stars show that the mass loss rates of young stars are much larger up to ~ 100 times of the present solar value (Wood et al. 2002, 2005).

Red giant stars also have surface convection zones. Alfvén waves possibly play a role in driving the stellar winds from red giant stars (e.g. Hartmann & MacGregor 1980; Holzer et al. 1983).

In this paper, we discuss stellar winds originating from surface convection zones. In particular we focus on how the mass loss rate is determined from the photospheric properties, based on our MHD simulations.

2 Our previous works for the present-day solar wind

In this section, we briefly summarize our MHD simulations for the solar wind. In Suzuki & Inutsuka (2005, 2006), we performed self-consistent one-dimensional (1D) simulations that handle the propagation, reflection, and dissipation of MHD waves in an individual super-radially open magnetic

* Corresponding author: e-mail: stakeru@nagoya-u.jp

¹ Recent steady-state calculations (e.g. Verdini & Velli 2007; Cranmer & van Ballegoijen 2007) also include the photosphere.

flux tube from the photosphere to the solar wind region. We took into account radiative cooling and thermal conduction to examine the coronal heating without ad hoc assumptions and three components of magnetic field and velocity to treat Alfvénwaves. We injected transverse fluctuations from the photosphere and run the simulations until the quasi-steady states were achieved. A main result of these papers is that the input of the transverse fluctuations with ~ 1 km/s at the photosphere naturally drives the solar wind which is observed today.

The Alfvénwaves which are excited from the photosphere are mostly reflected back downward because of the change of the Alfvén speed (Moore 1991), but roughly 10 % of the initial Poynting flux associated with the Alfvénwaves penetrates to the corona and contributes to the heating of the solar wind. The main channel of the dissipation of the Alfvén waves is the generation of compressive waves, particularly slow MHD waves (Kudoh & Shibata 1999). The steepening of the wave fronts leads to the shock dissipation of these excited compressive waves. In general, however, in the 1D simulations the shock dissipation tends to be overestimated because the waves are confined in the individual flux tubes without leakage.

In Matsumoto & Suzuki (2012), we extended to two dimensional (2D) simulations. The biggest difference is that we can treat the leakage of the waves to neighboring flux tubes. Cascading Alfvénic turbulence can be also handled, although it is restricted to the 2D space. In the 2D simulation, the effect of compressive waves is suppressed, while the turbulent cascade becomes comparably important in the dissipation of the Alfvénwaves. The overall dissipation rate of the Alfvénwaves is comparable to that of the 1D cases, and as a result, the 1D and 2D simulations give similar mass loss rates and terminal velocities.

In the following sections, we extend these simulations from the present-day solar wind to more active solar-type stars (§3) and red giant stars (§4). Because the 2D and 1D simulations yield similar global properties of the winds, we use the 1D simulations to save computational time.

3 Mass loss from young active solar-type stars

Young solar-type stars are generally very active. The X-ray flux is up to ~ 1000 times larger than the present Sun (e.g. Güdel 2004), and the transition region flux is also much larger (Ayres 1997). Observation of young main sequence stars show very strong magnetic fields with an order of kG or even larger (e.g., Donati & Collier Cameron 1997; Saar & Brandenburg 1999). The mass loss rate is also much higher but seems saturated around ~ 100 times of the present solar level (Wood et al. 2002; 2005).

In this section, we investigate how the solar atmosphere reacts to increases of magnetic field strength and fluctuation amplitude at the photosphere. As the reference case we set up a magnetic flux tube with field strength $B_0 = 1$ kG at the

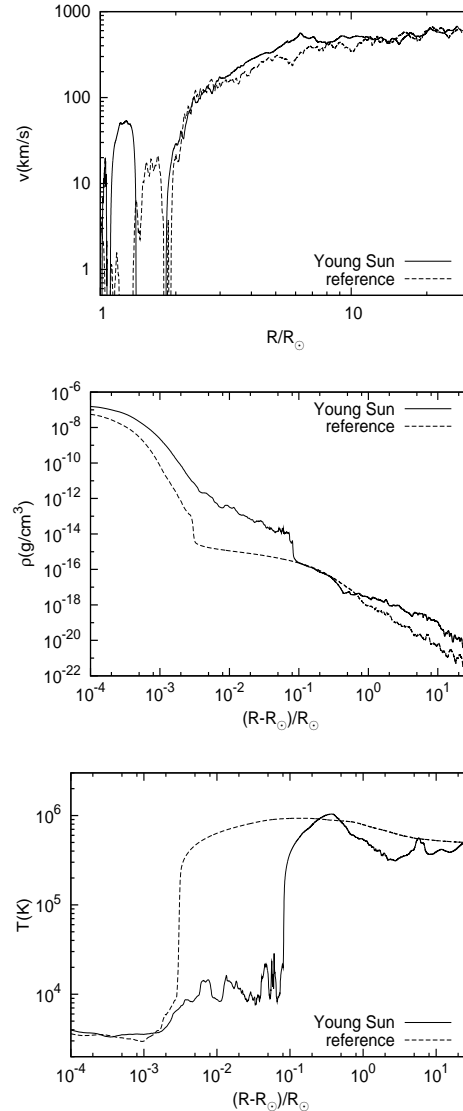


Fig. 1 Comparison of the wind structures. The solid lines are the wind structure for the active case (see text) and the dashed lines are the wind structure of the reference case. From top to bottom, velocity, density, and temperature are displayed.

photosphere and a super-radial expansion factor $f = 1000$ to match recent HINODE observations (Tsuneta et al. 2009; Ito et al. 2010), and inject fluctuations, $\delta v = 1.4$ km s $^{-1}$ from the photosphere. This reference case well reproduces the average global properties of the present-day solar wind. We perform more than 30 simulation runs with different B_0 , f , and δv .

Figure 1 shows the stellar wind structure which adopts $B_0 = 2$ kG, $\delta v = 2.8$ km s $^{-1}$, and $f = 1000$ (solid lines, labeled as ‘Young Sun’) in comparison with the reference case (dashed lines). This active case gives the mass loss rate, $\dot{M} = 4 \times 10^{-13} M_\odot/\text{yr}$, which is 20 times larger than $2 \times 10^{-14} M_\odot/\text{yr}$ obtained from the reference case (\approx the present value). Since the injected Poynting flux ($\propto B_0 \delta v^2$)

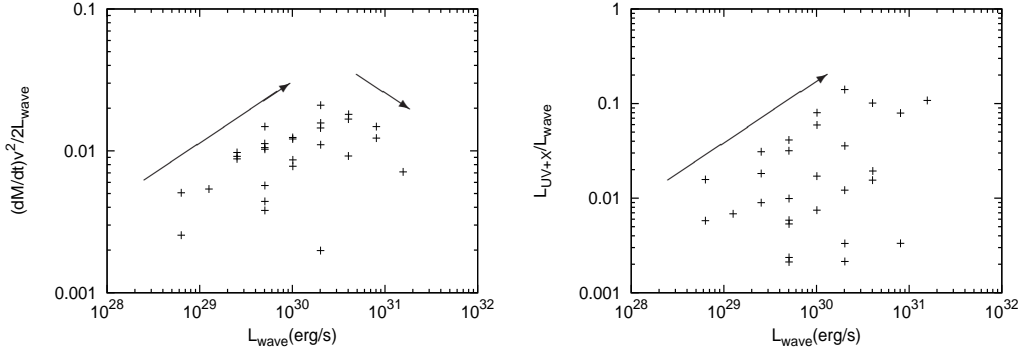


Fig. 2 Energetics of stellar wind derived from the simulations; each data point indicates each run. The left panel shows the fractions of the kinetic energy fluxes on the total input Poynting fluxes from the photospheres, and the right panel shows the fractions of the total radiative losses from the transition regions and coronae on the total input Poynting fluxes.

in the active case is only 8 times larger, the mass loss rate quite sensitively depends on the energy input. This is because of the global instability involved with the reflection and nonlinear dissipation of Alfvén waves (see Suzuki 2012 for details).

The location of the transition region in the active case is at $\approx 1.1 R_{\odot}$, which is much higher than the height of the transition region of the reference case ($\approx 1.003 R_{\odot}$). This is because in the active case more material is lifted up due to the larger energy injection from the photosphere and the temperature cannot increase easily owing to the larger radiative cooling. Hence, the chromosphere extends to higher altitude in the active case. Interestingly enough, the observation of a young solar-like star, CoRot-2a, by using the Rossiter-McLaughlin effect shows that this star possesses an extended chromosphere of up to 1.16 times of the stellar radius (Czesla et al. 2012).

Figure 2 displays the fractions of the kinetic energy flux of the stellar wind, $\dot{M} \frac{v^2}{2}$, (left) and the radiative loss from the transition region and corona (right) of each run against the total injected Poynting energy associated with Alfvén waves, L_{wave} , from the photosphere. Both panels show large scatters in the vertical direction, reflecting varieties of f . The sums of these two fractions are much less than unity in all the runs, because most of the input energies are reflected back downward.

The left panel shows that the fraction of the kinetic energy flux initially increases with increasing input energy; the increase of the kinetic energy of the stellar wind is more rapid than linear on the input energy, which is related with the global instability owing to the reflection and nonlinear dissipation of Alfvén waves as explained above (Suzuki 2012). However, it eventually saturates and decreases on increasing L_{wave} . On the other hand, the radiative loss shows saturation as well but the overturning trend is not so distinctive.

Combining these two panels, we can get the relation between radiative flux and mass loss rate (Fig. 3), which can be directly compared with the figures presented in Wood et

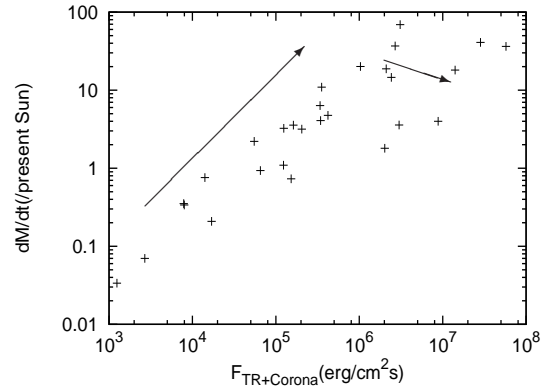


Fig. 3 Mass loss rate normalized by the present solar value on radiative flux from transition region and corona.

al. (2002, 2005). As expected from Fig. 2, the mass loss rate is positively correlated with radiative flux initially, while it eventually saturates, or even slightly decreases. The main reason of the saturation is that most of the input energies are exhausted for the radiative losses besides reflection in these saturated cases. Namely, the increase of \dot{M} is mainly done by the increase of density, which enhances radiative losses. Finally, no more energy remains for the kinetic energy of the stellar wind. We discuss this saturation mechanism in more detail in a forthcoming paper (Suzuki et al. 2012, in preparation).

4 Mass loss from red giants

After the hydrogen in the core is exhausted, a star evolves to a red giant stage. Because red giant stars have surface convection zones, it is expected that the fluctuations the surfaces would give a significant contribution to the stellar winds. On the other hand, the expansion of the radius largely affects the dynamics through the change of the surface gravity. We have carried out MHD simulations for red giant winds (Suzuki 2007), of which we briefly summarize the results.

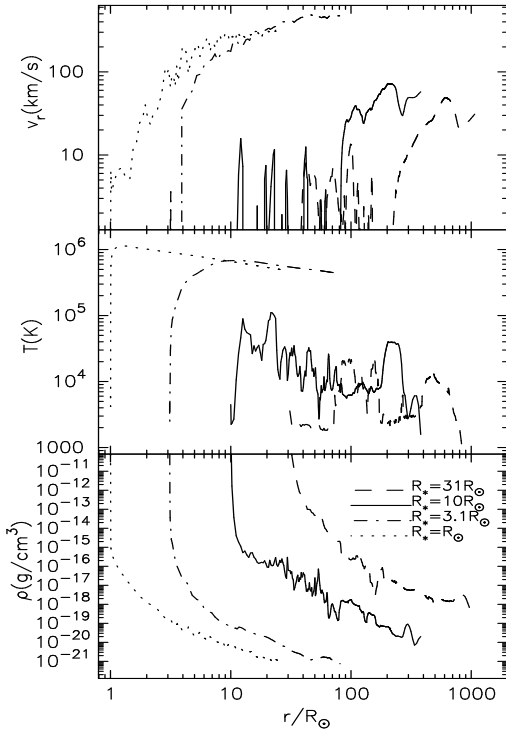


Fig. 4 From the top to the bottom, radial outflow velocity, v_r (km s^{-1}), temperature, T (K), and density, ρ (g cm^{-3}), are plotted. The dotted, dash-dotted, solid, and dashed lines are the results of stellar radii, $R = R_\odot$ (the present Sun), $3.1R_\odot$ (sub-giant), $10R_\odot$ (red giant), and $31R_\odot$ (red giant), respectively.

Figure 4 presents the evolution of stellar winds of a $1M_\odot$ star from main sequence to red giant stages. The surface amplitude is estimated from the convective flux (Renzini et al. 1977), whereas this should be tested by comparison with recently observed chromospheric fluxes (e.g. Pérez Martínéz et al. 2011). The middle panel shows that the average temperature drops suddenly from $T \simeq 7 \times 10^5 \text{ K}$ in the sub-giant star (dash-dotted) to $T \leq 10^5 \text{ K}$ in the red giant stars, which is consistent with the observed “dividing line” (Linsky & Haisch 1979). The main reason of the disappearance of the steady hot coronae is that the sound speed ($\approx 150 \text{ km s}^{-1}$) of $\approx 10^6 \text{ K}$ plasma exceeds the escape speed, $v_{\text{esc}}(r) = \sqrt{2GM_\star/r}$, at a few stellar radii in the red giant stars; the hot corona cannot be confined by the gravity any more in the atmospheres of the red giant stars. Therefore, the material flows out before heated up to coronal temperature as an extended chromosphere (Schröder & Cuntz 2005) with intermittent hot bubbles (Suzuki 2007; Crowley et al. 2008). In addition, the thermal instability of the radiative cooling function (Landini & Monsignori-Fossi 1990) plays a role in the sudden decrease of temperature; since the gas with $T = 10^5 - 10^6 \text{ K}$ is unstable, the temperature quickly decreases from the subgiant to red giants.

The densities of the winds increase with stellar evolution due to the decrease of the surface gravity. The wind velocities are much smaller than the surface escape speeds,

because the onset locations of the winds are around several stellar radii (Harper et al. 2009). Through the stellar evolution, the mass loss rate increases due to the increase of the stellar surface ($\propto R^2$) and the increase of the density. From the main sequence star to the red giant star with $R_\star = 31R_\odot$, the mass loss rate increases $10^5 - 10^6$ times.

Acknowledgements. This work was supported in part by Grants-in-Aid for Scientific Research from the MEXT of Japan, 22864006.

References

- Alazraki, G., Couturier, P.: 1971, *A&A*, 13, 380
 Axford, W.I., McKenzie, J.F.: 1992, *Solar Wind VII*, proc. of 3rd COSPAR coll., 1
 Ayres, T.R.: 1997, *JGR*, 102, 1641
 Belcher, J.W.: 1971, *ApJ*, 168, 509
 Cranmer, S.R., Saar, S.H.: 2011, *ApJ*, 741, 54
 Cranmer, S.R., van Ballegoijen, A.A., Edgar, R.J.: 2007, *ApJS*, 171, 520
 Crowley, C., Espey, B.R., McCandiss, S.R.: 2008, *ApJ*, 675, 711
 Czesla, S. et al.: 2012, *A&A*, 539, 150
 Donati, J.-F., Collier Cameron, A.: 2009, *ARA&A*, 47, 333
 Fujimura, D., Tsuneta, S.: 2009, *ApJ*, 702, 1443
 Güdel, M., Guinan, E.F., Skinner, S.L.: 1997, *ApJ*, 483, 947
 Harper, G.M. et al.: 2009, *ApJ*, 701, 1464
 Hartmann, L., MacGregor, K.B.: 1980, *ApJ*, 242, 260
 Hollweg, J.V.: 1973, *ApJ*, 181, 547
 Holzer, T.E., Fløa, T., Leer, E.: 1983, *ApJ*, 275, 808
 Ito, H., Tsuneta, S., Shiota, D., Tokumaru, M., Fujiki, K.: 2010, *ApJ*, 719, 131
 Kudoh, T., Shibata, K.: 1999, *ApJ*, 514, 493
 Kohl, J.L.: 1998, *ApJ*, 501, L127
 Landini, M., Monsignori-Fossi, B.C.: 1990, *A&AS*, 82, 229
 Linsky, J.L., Haisch, B.M.: 1979, *ApJ*, 229, L27
 Matthaeus, W.H., Zank, G.P., Oughton, S., Mullan, D.J., Dmitruk, P.: 1999, *ApJ*, 523, L93
 Matsumoto, T., Kitai, R.: 2010, *ApJ*, 716, L19
 Matsumoto, T., Suzuki, T.K.: 2012, *ApJ*, 749, 8
 Moore, R.L., Suess, S.T., Musielak, Z.E., An, A.-H.: 1991, *ApJ*, 378, 347
 Parker, E.N.: 1993, *ApJ*, 408, 707
 Pérez Martínéz, M.I., Schröder, K.-P., Cuntz, M.: 2011, *MNRAS*, 414, 418
 Renzini, A., Cacciari, C., Ulmschneider, P., Schmitz, F.: 1977, *A&A*, 61, 39
 Saar, S.H., Brandenburg, A.: 1999, *ApJ*, 524, 295
 Schröder, K.-P., Cuntz, M.: 2005, *ApJ*, 630, L73
 Suzuki, T.K.: 2007, *ApJ*, 659, 1592
 Suzuki, T.K.: 2012, *Earth, Planets, and Space*, 64, 201
 Suzuki, T.K., Inutsuka, S.: 2005, *ApJ*, 632, L49
 Suzuki, T.K., Inutsuka, S.: 2006, *JGR*, 111, A06101
 Tsuneta, S. et al.: 2008, *ApJ*, 688, 1374
 Verdini, A., Velli, M.: 2007, *ApJ*, 662, 669
 Wood, B.E., Müller, H.-R., Zank, G.P., Linsky, J.L.: 2002, *ApJ*, 574, 412
 Wood, B.E., Müller, H.-R., Zank, G.P., Linsky, J.L., Redfield, S.: 2002, *ApJ*, 628, L143
 Yoshimura, H.: 1975, *ApJS*, 201, 740